AD-A119 331 NAVAL POSTGRADUATE SCHOOL MONTEREY CA F/G 4/2
SINGLE-STATION ASSESSMENTS OF THE SYNOPTIC-SCALE FORCING ON THE--ETC(U)
JUN 82 J P GLEASON

UNCLASSIFIED NL

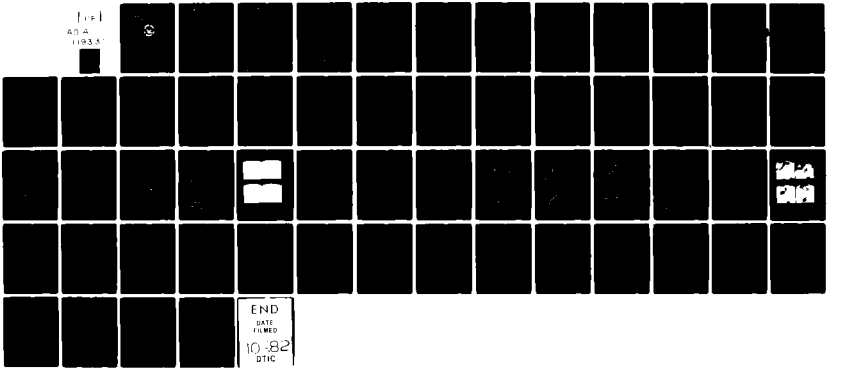

NAVAL POSTGRADUATE SCHOOL
Monterey, California

SINGLE-STATION ASSESSMENTS OF THE SYNOPTIC-SCALE FORCING ON THE MARINE ATMOSPHERIC BOUNDARY LAYER

by

John Patrick Gleason

June 1982

Thesis Advisor: K. L. Davidson

Approved for public release; distribution unlimited.

SECURITY CLASSIFICATION OF THIS PAGE (When Data Entered)

REPORT DOCUMENTATION PAGE		READ INSTRUCTIONS BEFORE COMPLETING FORM
1. REPORT NUMBER	2. GOVT ACCESSION NO. AD-A119331	3. RECIPIENT'S CATALOG NUMBER
4. TITLE (and Subtitle) Single-Station Assessments of the Synoptic-Scale Forcing on the Marine Atmospheric Boundary Layer		5. TYPE OF REPORT & PERIOD COVERED Master's Thesis June 1982
		6. PERFORMING ORG. REPORT NUMBER
7. AUTHOR(s) JOHN P. GLEASON		8. CONTRACT OR GRANT NUMBER(s)
9. PERFORMING ORGANIZATION NAME AND ADDRESS Naval Postgraduate School Monterey, California 93940		10. PROGRAM ELEMENT, PROJECT, TASK AREA & WORK UNIT NUMBERS
11. CONTROLLING OFFICE NAME AND ADDRESS Naval Postgraduate School Monterey, California 93940		12. REPORT DATE June 1982
		13. NUMBER OF PAGES 57
14. MONITORING AGENCY NAME & ADDRESS(if different from Controlling Office)		15. SECURITY CLASS. (of this report)
		15a. DECLASSIFICATION/DOWNGRADING SCHEDULE

16. DISTRIBUTION STATEMENT (of this Report)

Approved for public release; distribution unlimited.

17. DISTRIBUTION STATEMENT (of the abstract entered in Block 20, if different from Report)

18. SUPPLEMENTARY NOTES

19. KEY WORDS (Continue on reverse side if necessary and identify by block number)

Single-station assessment
Single-station forecasting
Vertical velocity
Atmospheric Planetary Boundary Layer
Adiabatic Method
Kinematic Method
Q-method

20. ABSTRACT (Continue on reverse side if necessary and identify by block number)

Knowledge of the large-scale vertical velocity is required to predict the evolution of the atmospheric planetary boudary layer (APBL). Since naval operations are often conducted in data sparse regions, single-station assessments of the vertical velocity are necessary. Data to evaluate such assessments were obtained from rawinsondes taken at San Nicolas Island, California. Vertical velocity estimates obtained by vertical integration of

(CONTINUED)

DD FORM 1 JAN 73 1473 EDITION OF 1 NOV 65 IS OBSOLETE
S/N 0102-014-6601

SECURITY CLASSIFICATION OF THIS PAGE (When Data Entered)

20. ABSTRACT (continuation).

the moisture budget equation (Q-method) and by the adiabatic method were used to initialize an APBL 24-hour prediction model. RMS error statistics on predicted inversion height, potential temperature, and specific humidity were computed for the forecasts and compared to the RMS errors of a persistence forecast. Calculation of the vertical velocity by the Q-method showed the most promise. However, no single-station assessment method improved on the persistence forecasts.

Approved for public release; distribution unlimited

Single-Station Assessments of the Synoptic-Scale Forcing on the Marine Atmospheric Boundary Layer

by

John P. Gleason
Lieutenant, United States Navy
B.S., University of Utah, 1976

Submitted in partial fulfillment of the
requirements for the degree of

MASTER OF SCIENCE IN METEOROLOGY AND OCEANOGRAPHY

from the

NAVAL POSTGRADUATE SCHOOL
June 1982

Author: John P. Gleason

Approved by: Kenneth L. Davidson
Thesis Advisor

Gordon E. Schacher
Second Reader

Chairman, Department of Meteorology

William M. Tolles
Dean of Science and Engineering

ABSTRACT

Knowledge of the large-scale vertical velocity is required to predict the evolution of the atmospheric planetary boundary layer (APBL). Since naval operations are often conducted in data sparse regions, single-station assessments of the vertical velocity are necessary. Data to evaluate such assessments were obtained from rawinsondes taken at San Nicolas Island, California. Vertical velocity estimates obtained by vertical integration of the moisture budget equation (Q-method) and by the adiabatic method were used to initialize an APBL 24-hour prediction model. RMS error statistics on predicted inversion height, potential temperature, and specific humidity were computed for the forecasts and compared to the RMS errors of a persistence forecast. Calculation of the vertical velocity by the Q-method showed the most promise. However, no single-station assessment method improved on the persistence forecasts.

TABLE OF CONTENTS

LIST OF FIGURES

LIST OF TABLES

ACKNOWLEDGEMENT

I wish to thank:

- Professor K.L. Davidson for his guidance and encouragement.
- Dr. C.W. Fairall, B.D.M. Corporation, for taking time with me to discuss many aspects of the thesis.
- Professor G.E. Schacher for his review of the thesis.
- Mr. Jay Rosenthal of the Geophysics Division, Pacific Missile Test Center, for providing the rawinsonde and surface observation data, and for his enthusiastically expressed interest in the thesis.
- Ms. Pat Boyle for her assistance in programming and research.

Special thanks are reserved for Bonnie, Johanna and Andrea.

I. INTRODUCTION

One aspect of naval operations is battle group operations in a fixed geographical area. This is currently referred to as MODLOC. Several scenarios lend themselves to MODLOC operations: the Viet-Nam era carrier based strike operations, pre-positioning for a projection of power, or simply a show of force. Training operations, as well, are often conducted in fixed areas to avoid hazards to commercial shipping and air traffic with weapons firings, or for privacy in operations.

A second aspect is the need for self sufficiency of a deployed force. Any autonomous ability to make environmental prediction within the battle group reduces the requirements for shorebased support, decreases delivery time for perishable information and reduces the demand on communication assets.

A third aspect is the effect of the atmosphere on the perfcrmance of weapons and sensors that depend on electromagnetic and electro-optical wave propagation. Meteorological factors which affect such propagation can change significantly in four to six hours. The importance of APBL prediction to naval operations lies in:

- Prediction of the existence and evolution of electromagnetic ducts.
- Prediction of the inversion height, where it is known that optical propagation is degraded due to turbulence.

This thesis is an examination of the accuracy of single-station assessments of the large-scale vertical velocity, and the effectiveness of these assessments for an existing APBL prediction model. Three methods of computing the vertical velocity will be discussed. Vertical velocities calculated by single-station methods will be used in an APBL model to ascertain the relative merits of these methods.

II. BACKGROUND

The single-station forecasting problem probably has been of interest as a military requirement since the origin of armed conflict. Oliver and Oliver (1945) put single-station assessments into a naval perspective:

> During the last few years, wartime conditions have made it necessary for isolated combat units to issue forecasts in regions where no network of meteorological stations could be available. Frequently the data from several stations or from reconnaissance planes are available, but in some regions the forecaster must rely only on surface and upper-air observations made at his own station. This is particularly true in the case of ships at sea. Hence, it is important to develop proficiency at extracting information with limited aerological data.... He must further be able to distinguish from solutions which are internally consistent, and those which are inconsistent and therefore to be discarded.

In APBL assessments the assumption of horizontal homogeneity (one-dimensionality) is often used. All APBL prediction models require, as an externally known parameter, the large-scale vertical velocity which direcly affects changes in the height of the APBL. Furthermore, the height of the APBL affects other properties of the boundary layer such as the temperature and humidity.

Data for this examination were obtained from rawinsondes taken at San Nicolas Island (SNI), California. SNI data are sufficiently representative of a marine environment for this

purpcse. Battalino et al. (1979) have stated that conditions at SNI may be marine, continental, or mixed depending on the circulatien patterns. A decision to use the SNI data was made, in part, because of the availability of similar data from Vandenberg (VND) Air Force Base, California and Point Mugu (PMTC), California, so that examination of the horizontal variability of the area and divergence derived vertical velocity values could be accomplished. Fig. 1 is provided for geographic orientation.

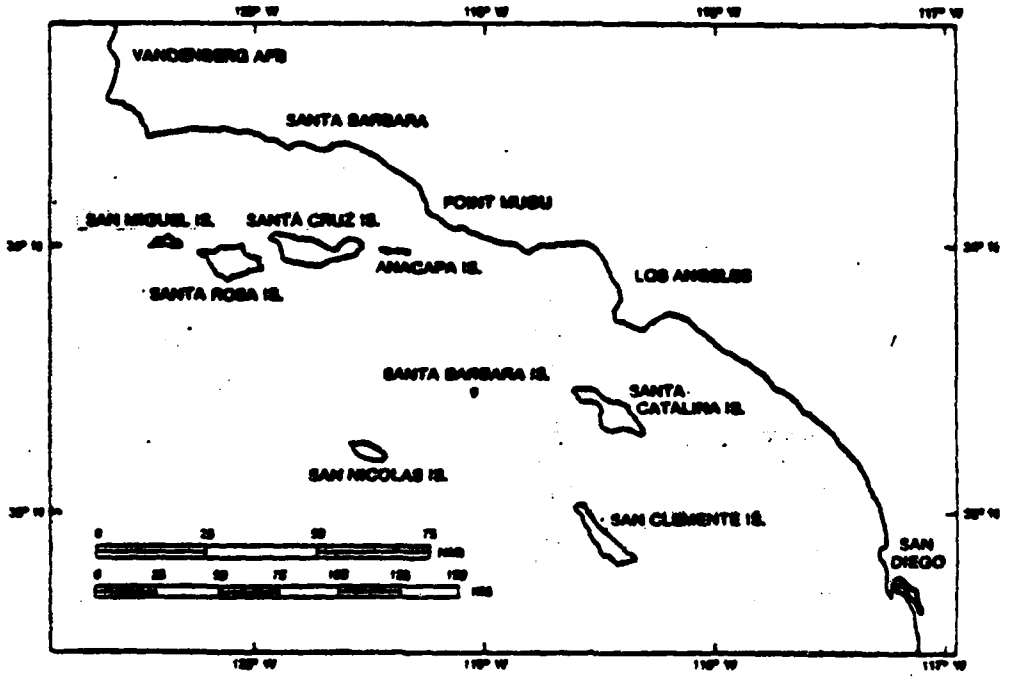

Figure 1. Southern California Coastal Waters. (After Battalino et al. 1979.)

A. THE PREDICTION MODEL

An APBL prediction model in which the mean vertical motion is an external parameter is used to establish the affect of the derived values of vertical velocity on boundary layer evolution. The model used is based on the one presented by Stage and Businger (1981) and was coded for operational use by Brower (1982). The predictive equations are:

$$dq/dt = h^{-1}(\overline{w'q'}(0) + W_e \Delta q) \quad (1a)$$

$$d\theta_e/dt = h^{-1}(\overline{w'\theta_e'}(0) + R_c - R_b + W_e \Delta\theta_e) \quad (1b)$$

$$dh/dt = W_D + W_e \quad (1c)$$

Where q is the total water content (liquid and vapor), h is the inversion height, θ_e is the equivalent potential temperature, $\overline{w'q'}(0)$ is the surface flux of moisture, $\overline{w'\theta_e'}(0)$ is the surface buoyancy flux, Δ is the difference between the variable value immediately above the APBL and its well mixed value in the APBL, R_c is the rate of radiative heat gain per unit area at the cloud base, and R_b is the rate of radiative heat loss per unit area near the cloud top. W_e is the entrainment velocity and W_D is the large-scale vertical velocity at the inversion height.

The model atmosphere is two layered, composed of a turbulent lower layer in which equivalent potential temperature, specific humidity and wind speed are constant with height, and a stable upper atmosphere with constant specific humidity and buoyancy gradients. The layers are separated at the inversion height by a zero-order discontinuity (jump). Fig. 2 depicts how a sample sounding is characterized in the model atmosphere.

Surface fluxes of moisture and bouyancy are diagnosed from bulk formulae (Lilly 1968). The liquid water profile is computed adiabatically and reduced by about 30 percent to agree with empirical results (Fairall et al. 1981.) Long wave radiative cooling is treated using the Stephan-Boltzman law, and short wave radiative warming is treated using the delta-Eddington approximation (Fairall et al. 1981).

The large-scale vertical velocity, W_D , is treated as an external parameter, and is constant over the model run (24-hr). The system is closed with the specification of the entrainment velocity which is accomplished by the assumption that dissipation of turbulent kinetic energy (TKE) is a fixed fraction of the production of TKE (Stage and Businger 1981). A 30-minute time step is used.

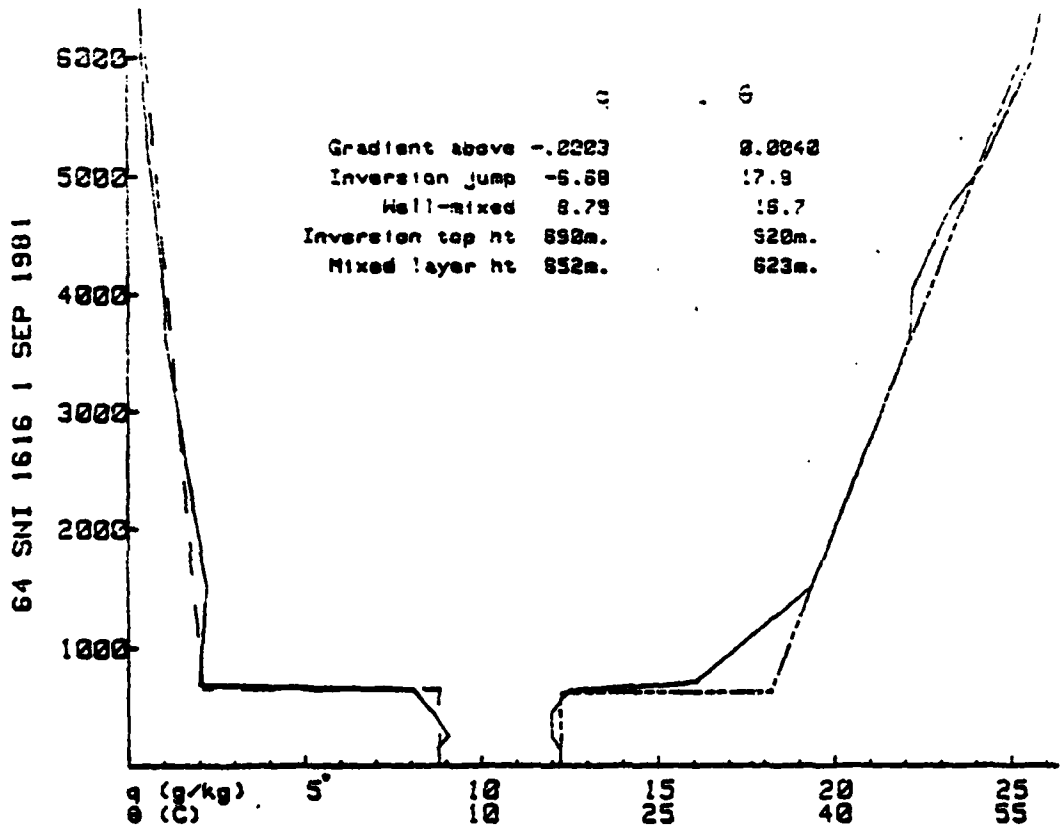

Figure 2. Sample sounding in the model atmosphere. Solid line represents data, dashed line represents the model atmosphere.

III. METHODS

At least three methods which can be used to compute the large-scale vertical velocity are:

- The kinematic method.
- The adiabatic method.
- Integration of the moisture budget equation.

The kinematic method requires wind sounding data from at least three appropriately spaced stations. The adiabatic method and the integration of the moisture budget equation are truly single-station assessments.

A. THE KINEMATIC METHOD

The kinematic method can be used to compute the vertical velocity when nearly simultaneous (within two hours) soundings are available at three or more appropriately spaced stations such as VND, PMTC, and SNI (Fig. 1). Following Saucier (1955), the vertical velocity can be derived:

$$\partial w/\partial z = -(\partial u/\partial x + \partial v/\partial y), \qquad (2)$$

where u, v and w are the zonal, meridional and vertical wind components. The horizontal wind components can be linearly approximated by a Taylor series expansion as:

$$u = u_o + (\partial u/\partial x)\, x + (\partial u/\partial y)\, y, \qquad (3a)$$

$$v = v_o + (\partial v/\partial x)\, x + (\partial v/\partial y)\, y. \qquad (3b)$$

Eq. (3) suggests that the horizontal derivatives may be obtained from a regression of the horizontal wind components onto the horizontal plane (Fairall et al. 1981). Decomposition of the wind vector from the sounding data at the three stations (SNI, VND, PNTC) into zonal and meridional components is required. Vertical profiles of the horizontal wind components were constructed at a 200 meter vertical increment by linear interpolation from the irregularly spaced data levels to those levels that are an integer multiple of 200 meters. Multiple linear regression of each component of the horizontal wind onto the horizontal plane is performed as follows:

$$u = a + bx + cy, \qquad (4a)$$

$$v = d + ex + fy, \qquad (4b)$$

where a through f are the regression coefficients.

Comparison of Eq. (3) with Eq. (4) indicates that the coefficients b and f give the zonal derivative of zonal wind and the meridional derivative of meridional wind at the center of a triangle formed by the three locations and at each vertical level where the regression is done.

Vertical integration of Eq. (2) is performed to give a vertical profile of vertical velocity to three kilometres:

$$w(z) = - \sum^{3km} ((b) + (f)) \Delta z , \qquad (5)$$

where $w(z=0) = 0$ and $\Delta z = 200$m.

B. THE ADIABATIC METHOD

For isentropic motions there is no time change of potential temperature following the motion. Based on this assumption Saucier (1955) specifies the adiabatic method for estimating vertical velocity as:

$$w = - \frac{(\partial\theta/\partial t) + V \cdot (\nabla\theta)}{(\partial\theta/\partial z)} \quad , \qquad (6)$$

where θ is the potential temperature. Saucier further states that the local temperature change due to advection may be on the order of that due to vertical motion. In this study, calculations of vertical velocity are made both including and neglecting the advective term. Description of the advection calculation is left to a subsequent section.

The vertical gradient is determined by a linear fit to the lapse rate of potential temperature above the inversion. The local time change of temperature is obtained at fixed heights ($z = 1.0, 1.25, 1.5$ km) from sequential soundings at the same location. These heights are above the inversion. It is assumed that the vertical velocity at the surface is zero. The vertical velocity at the inversion is taken as the average of the vertical velocity at the fixed heights

linearly scaled to the inversion height. Thus, a single-station assessment of the vertical velocity is obtained.

C. INTEGRATION OF THE MOISTURE BUDGET

Integration of the moisture budget equation to compute the vertical velocity was performed by Lenschow (1973). This method will hereafter be referred to as the Q-method, and is based on the assumption of well-mixed specific humidity in the boundary layer, and that changes occur due to fluxes at the sea surface and inversion only.

Vertical integration of the moisture budget equation through the boundary layer and across the interface between boundary layer and the stable atmosphere above yields the follcwing expression for vertical velocity, w, at the level of the inversion, h:

$$w = \frac{\Delta(q+l)\,(dh/dt) - h(d(q+l)/dt) + \overline{w'q'}(0)}{\Delta(q+l) + (\beta h/2)}, \qquad (7)$$

where q and l are vapor and liquid water contents, $\overline{w'q'}$ is the moisture flux, β is the vertical gradient of (q+l) in the mixed layer, and $\Delta(q+l)$ is the difference between total moisture in the mixed layer and total moisture immediately above the mixed layer. With no liquid water, $z \ll h$, and neglecting moisture advection Eq. (7) is simplified to:

$$w = \frac{\Delta q\,(dh/dt) - h\,(dq/dt) + \overline{w'q'}(0)}{\Delta q} \quad . \qquad (8)$$

Lilly (1968) assumes that β is zero. Lenschow (1973) found $\beta h/2$ to be small and certainly much less than the moisture jump.

Eq. (8) provides another independent assessment of the vertical velocity at the inversion. The time derivatives (dh/dt and dq/dt) are determined from sequential soundings. The moisture jump and inversion height are taken as averages for the two soundings, and the surface moisture flux is determined by the bulk method, i.e.,

$$\overline{w'q'}(0) = C_h V_{10}(q_s - q_{10}) \qquad (9)$$

The exchange coefficient, C_h, is computed from the wind speed dependent relation of Large and Pond (1980). The surface specific humidity, q_s, is determined via Tetens' formula for the vapor pressure (Buck 1981).

D. DETERMINATION OF ADVECTION FROM THE THERMAL WIND

Under the geostrophic assumption, the horizontal temperature gradient is directly proportional to the vertical shear of geostrophic wind. Following Byers (1974):

$$v = f^{-1}(\partial\phi/\partial x)_p \quad ; \quad u = -f^{-1}(\partial\phi/\partial y)_p \,, \qquad (10)$$

where v and u are the meridional and zonal components of the geostrophic wind, f is the Coriolis parameter, ϕ is the geopotential and the horizontal derivatives are on the constant pressure surface. Vertical differentiation of Eq. (10) and substitution from the hydrostatic equation yields:

$$\partial v/\partial p = f^{-1}(-\alpha) , \qquad (11a)$$

$$\partial u/\partial p = f^{-1}(\alpha) , \qquad (11b)$$

where α is the specific volume. Substitution from the equation of state and rearranging terms, the components of the temperature gradient are:

$$(\partial T/\partial x)_p = -(fp/R)(\partial v/\partial p) , \qquad (12a)$$

$$(\partial T/\partial y)_p = (fp/R)(\partial u/\partial p) , \qquad (12b)$$

where R is the gas constant for dry air.

With a wind sounding, assumed to be geostrophic above the boundary layer, the horizontal temperature gradient can be specified and a single-station assessment of the thermal advection term in Eq. (6) is obtained: $-(V\cdot\nabla T)=-(V\cdot\nabla\theta)$, at a constant level.

This calculation is performed by subtracting the wind at the first level above the inversion from the wind at an upper level. The advecting wind is the mean wind in the layer.

E. SINGLE-STATION ASSESSMENT SCORES

The separate vertical velocities computed from single-station assessments by the adiabatic method and the Q-method were both used as the large-scale vertical velocity in the APBL model.

Both methods required use of finite differences in time to approximate time derivatives. The time increment used was the time difference between subsequent soundings at SNI; it varied from four to eighteen hours. To establish the vertical velocity for a model run, the time weighted average vertical velocity was used, as computed from the SNI data for the 24 hour period following model initialization.

The model requires initial values of inversion height, and initial profiles of potential temperature and specific humidity. Sea surface temperature, required for computing surface moisture flux, was constant through the model day. Wind speed, required for computing surface moisture and bouyancy fluxes, was input as a linearly changing function of time.

Three model runs were made on each set of initial conditions: one with vertical velocity by the Q-method, a second with vertical velocity by the adiabatic method and the last

with vertical velocity set to zero. The advective term of Eq. (6) it was found to be much less than the local time change of potential temperature. Thus, it was neglected.

Root Mean Square (RMS) error was computed for predicted inversion height, h, potential temperature, θ, and specific humidity, q.

$$\text{RMS error} = \frac{1}{N}\left\{\sum_{i=1}^{N}(x_i - y_i)^2\right\}^{1/2},$$

where N is the number of observations, x_i is the observed value of a variable, and y_i is the predicted value of a variable. Observed values were obtained from rawinsonde data available within the 24 hours following the time of the initial data. Typically, two or three soundings were available for each 24-hour period following initialization. Predicted values were taken from the model output for the time corresponding to that of the observed values (± 15 minutes, due to the 30 minute model time step).

IV. SYNOPTIC SITUATION

Two periods (cases) were considered. Case I was from 31 August to 4 September 1981 and consisted of the analyses of nine model predictions verified against twenty observations. Case II was from 15 to 18 September 1981 and consisted of the analyses of eight predictions verified against seventeen observations.

A. CASE I (31 AUG - 4 SEPT 1981)

Throughout the period the eastern North Pacific Ocean was under a high pressure system that was moving slowly eastward. Southern California was dominated by a thermal trough, leading to weak offshore flow at the surface, while California was to the south of the strongest westerlies at upper levels. Figs. 3 through 6 show the National Meteorological Center (NMC) surface and 500 millibar (mb) analyses for Case I.

Selected prints of the GOES WEST Infra-red (IR) imagery indicate low broken to overcast cloudiness in the vicinity of SNI (Fig. 7). Surface observations at SNI indicated overcast conditions with fog at night, and scattered low

cloudiness with haze persisting after the late morning burn-off of the fog.

A Pacific high pressure system dominated the eastern ocean area west of California on 31 August (Fig. 3). A low pressure system was located in the Gulf of Alaska with its associated weak frontal system. Tropical Storm Irwin was dissipating southwest of the Baja Peninsula. A thermal trough dominated the central California valley. Very weak westerly flow aloft was predominant over southern California and most of the eastern Pacific Ocean.

After 31 August the Pacific high intensified, while the low pressure system in the Gulf of Alaska moved into the northwest United States and the assosiated cold front dissipated. The thermal trough over inland California moved slightly eastward and dominated the high desert region of Arizona and southeastern California (Figs. 4 through 6). Flow aloft remained very weak over southern California and the low level flow in the vicinity of SNI was very weak (3 to 5 kt) and predominantly offshore.

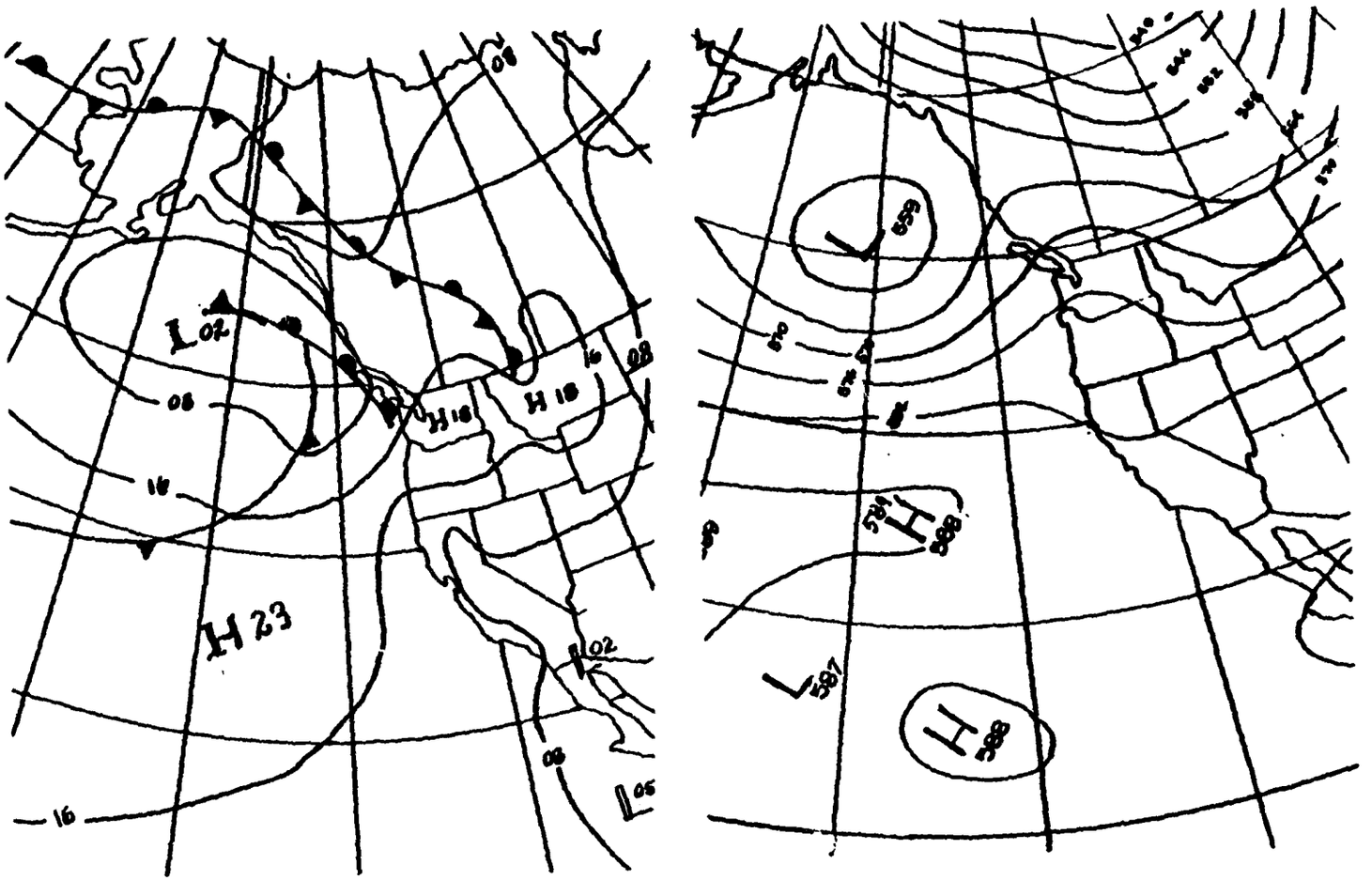

Figure.3. Surface and 500 mb analyses, 1200 GMT 31 Aug 1981.

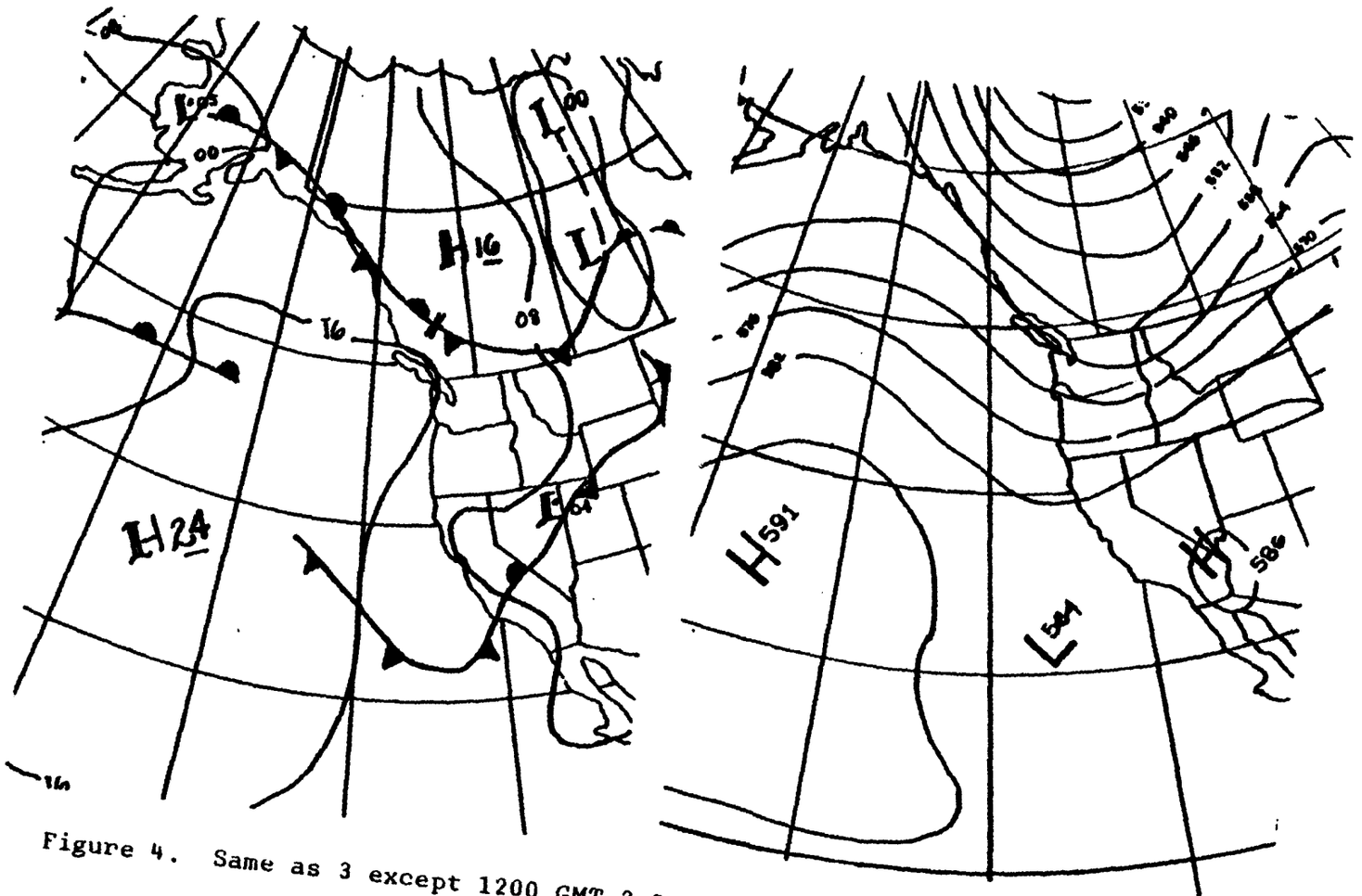

Figure 4. Same as 3 except 1200 GMT 2 Sept 1981.

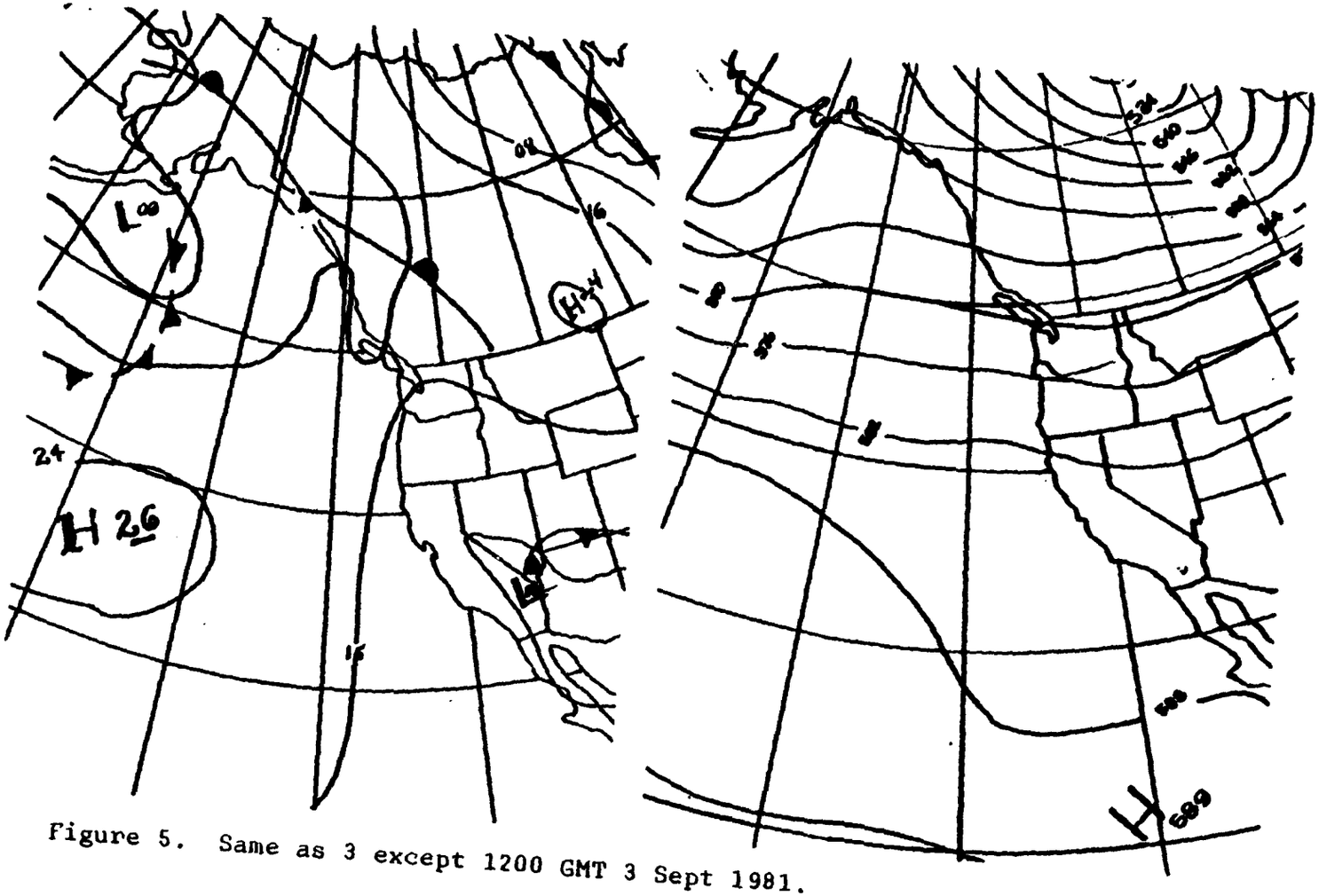

Figure 5. Same as 3 except 1200 GMT 3 Sept 1981.

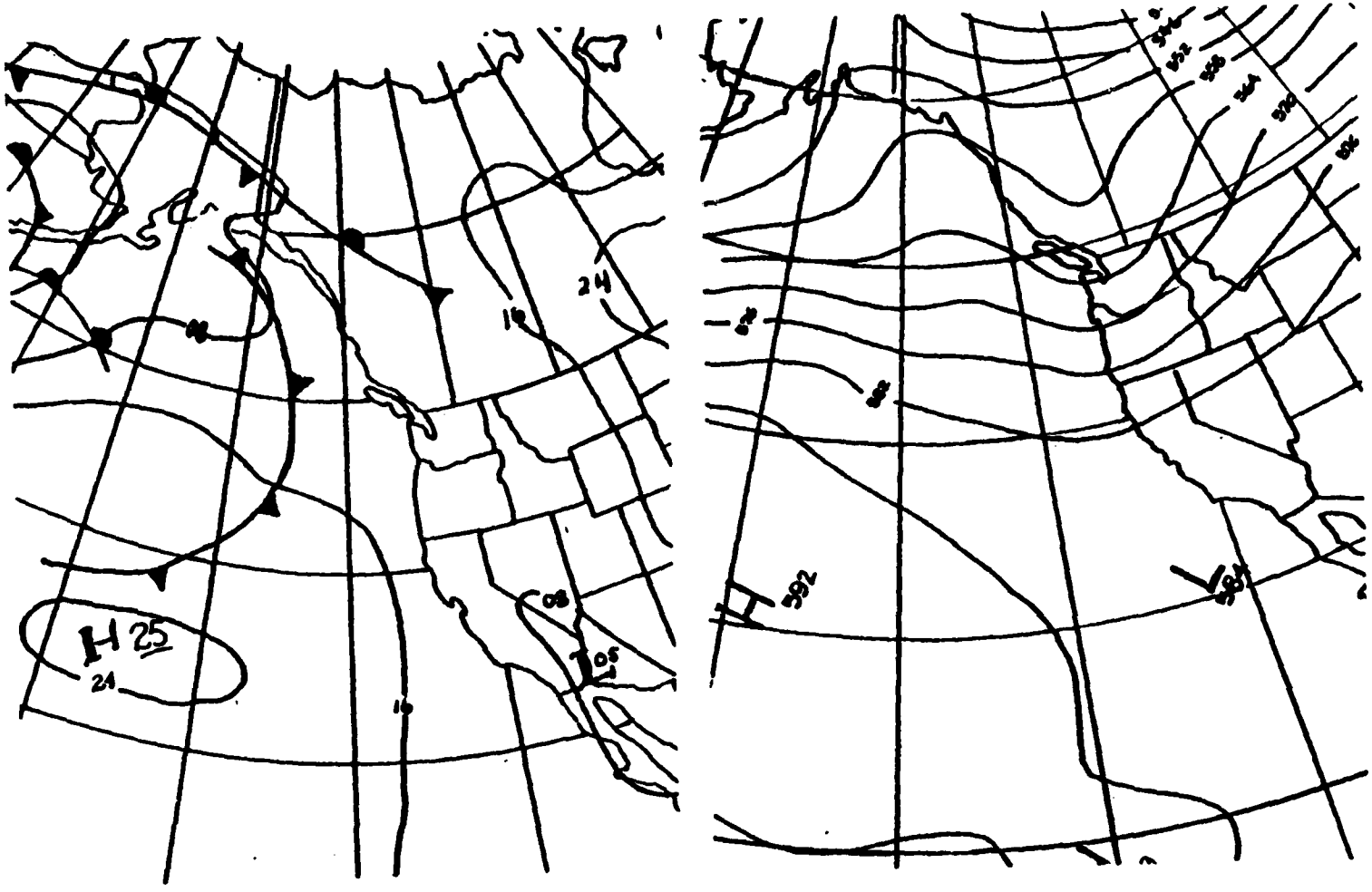

Figure 6. Same as 3 except 1200 GMT 4 Sept 1981.

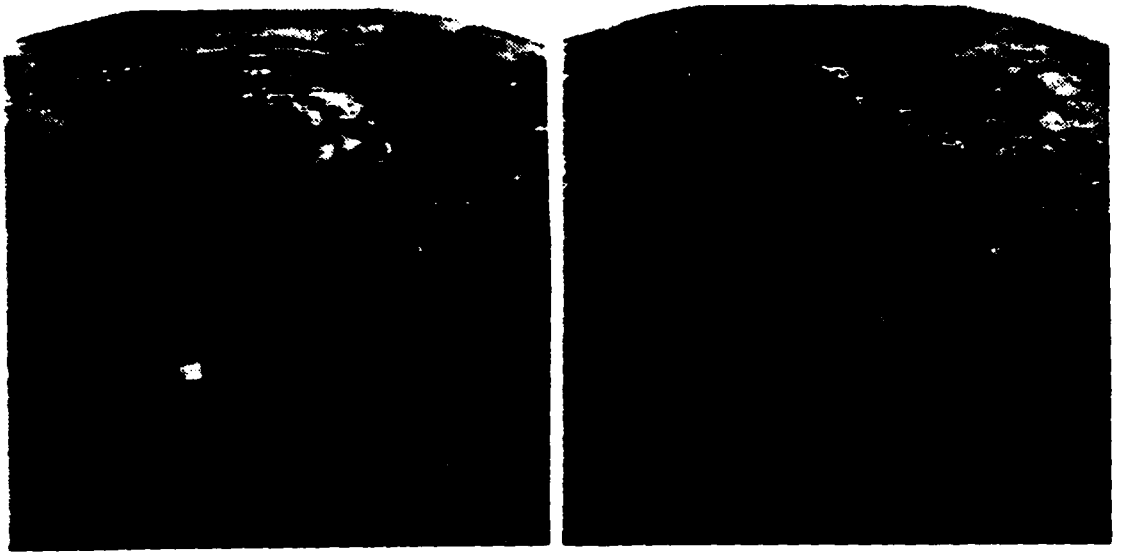

1245 GMT 31 AUG 81 1315 GMT 1 SEP 81

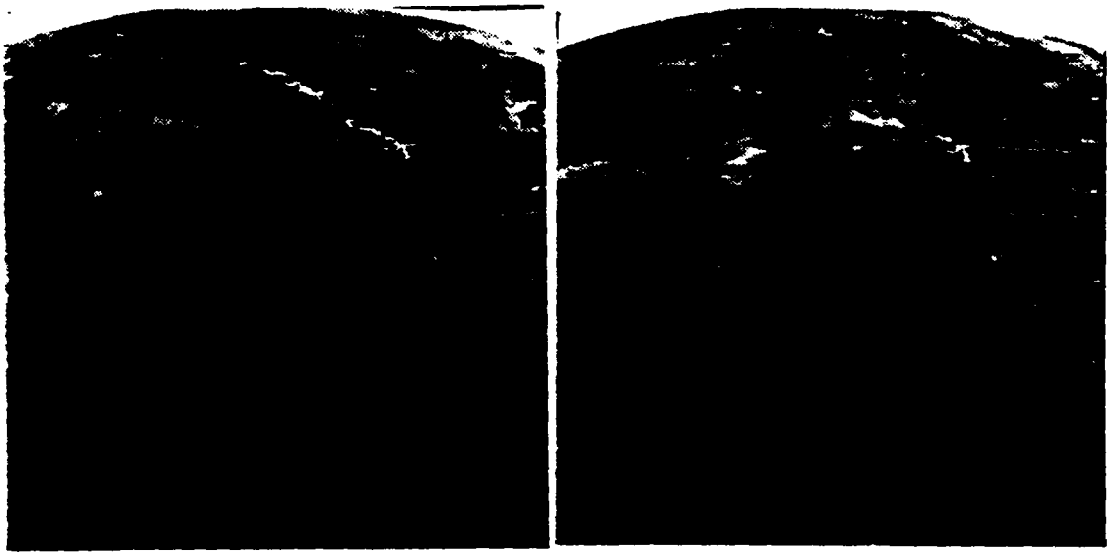

1245 GMT 2 SEP 81 1315 GMT 3 SEP 81

Figure 7. GOES WEST IR, CASE I.

B. CASE II (15-18 SEPT 1981)

Throughout the period the polar front was located in the eastern part of the North Pacific Ocean and Gulf of Alaska. A high pressure system dominated the area southeast of the polar front. A thermal trough was located over the inland California valley and through much of the southwestern United States and Mexico. Figs. 9 through 13 show the NMC surface and 500 mb analyses for Case II.

Satellite imagery indicates considerable clear area in the vicinity of SNI. Surface observations at SNI reported scattered low and high clouds with occasional reduced visibility due to fog and haze. Selected prints of the GOES WEST IR imagery are shown in Fig. 14 .

On 14 September high pressure prevailed over the eastern Pacific Ocean. The thermal trough dominated the southwestern United States and the Mexican Plateau. A low pressure system with a weak frontal system existed in the Gulf of Alaska. Weak unorganized flow existed south of the strongest westerlies in a large region of very flat height gradients over most of California and the eastern Pacific Ocean (Fig. 9).

By 15 September a large amplitude ridge aloft had built over the western United States and Canada (Fig. 10). The thermal trough weakened in central California as the ridge axis in the eastern Pacific Ocean migrated eastward. Low level flow in southern California was offshore and stronger (12 to 22 kt) than in Case I.

C. DIFFERENCES BETWEEN CASES I AND II

Comparison of the mixed layer and overlying data clearly indicates that different synoptic situations existed for the two cases. These differences are summarized in Table I and illustrated in Fig. 8 :

TABLE I

Comparison of the two cases

	Case I	Case II
mean h	604 m	262 m
range of h	511 to 667 m	145 to 357 m
mean θ	16.2 C	18.1 C
mean $\Delta\theta$	15.0 C	14.1 C
mean q	8.3 g/kg	9.8 g/kg
mean Δq	-6.0 g/kg	-4.4 g/kg
mean $\partial\theta/\partial z$ above h	4.2 C/km	2.8 C/km
mean $\partial q/\partial z$ above h	-.35 g/(kg-km)	-.83 g/(kg-km)

On the average, inversion height was nearly 2.5 times greater in Case I than in Case II. Case II had a warmer and more moist boundary layer with smaller magnitudes of jumps

in both potential temperature and specific humidity. The vertical gradient of potential temperature (stability) above the inversion is 1.5 times greater in Case I than Case II, and the vertical moisture gradient is nearly 2.5 times larger in Case I than Case II.

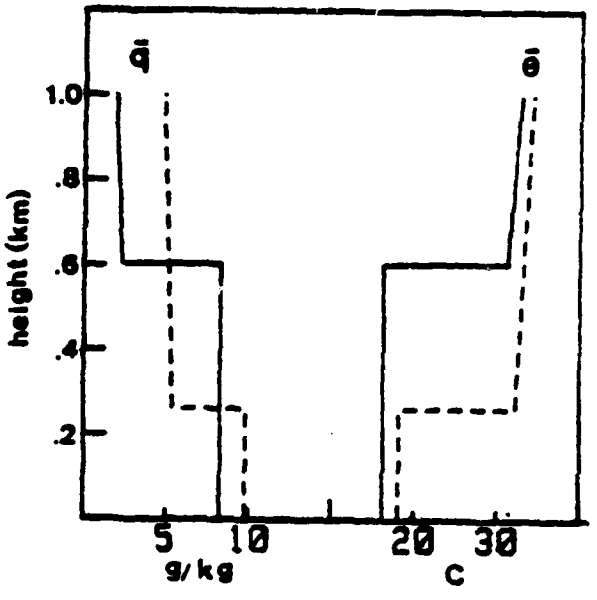

Figure 8. Average Model Atmosphere: Case I vs. Case II
Solid: Case I, dash: Case II

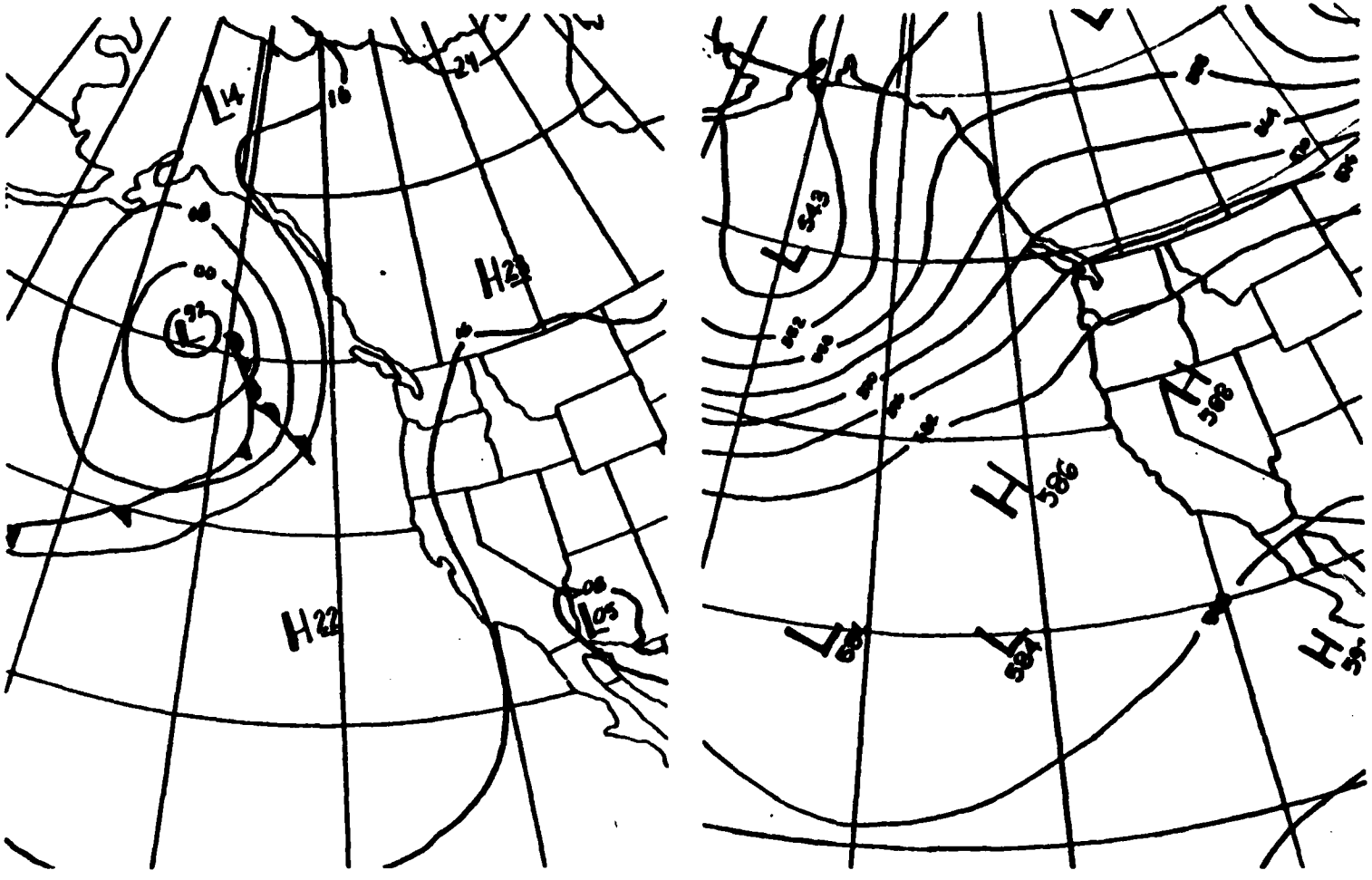

Figure 9. Surface and 500 mb analyses, 0000 GMT 14 Sept 1981.

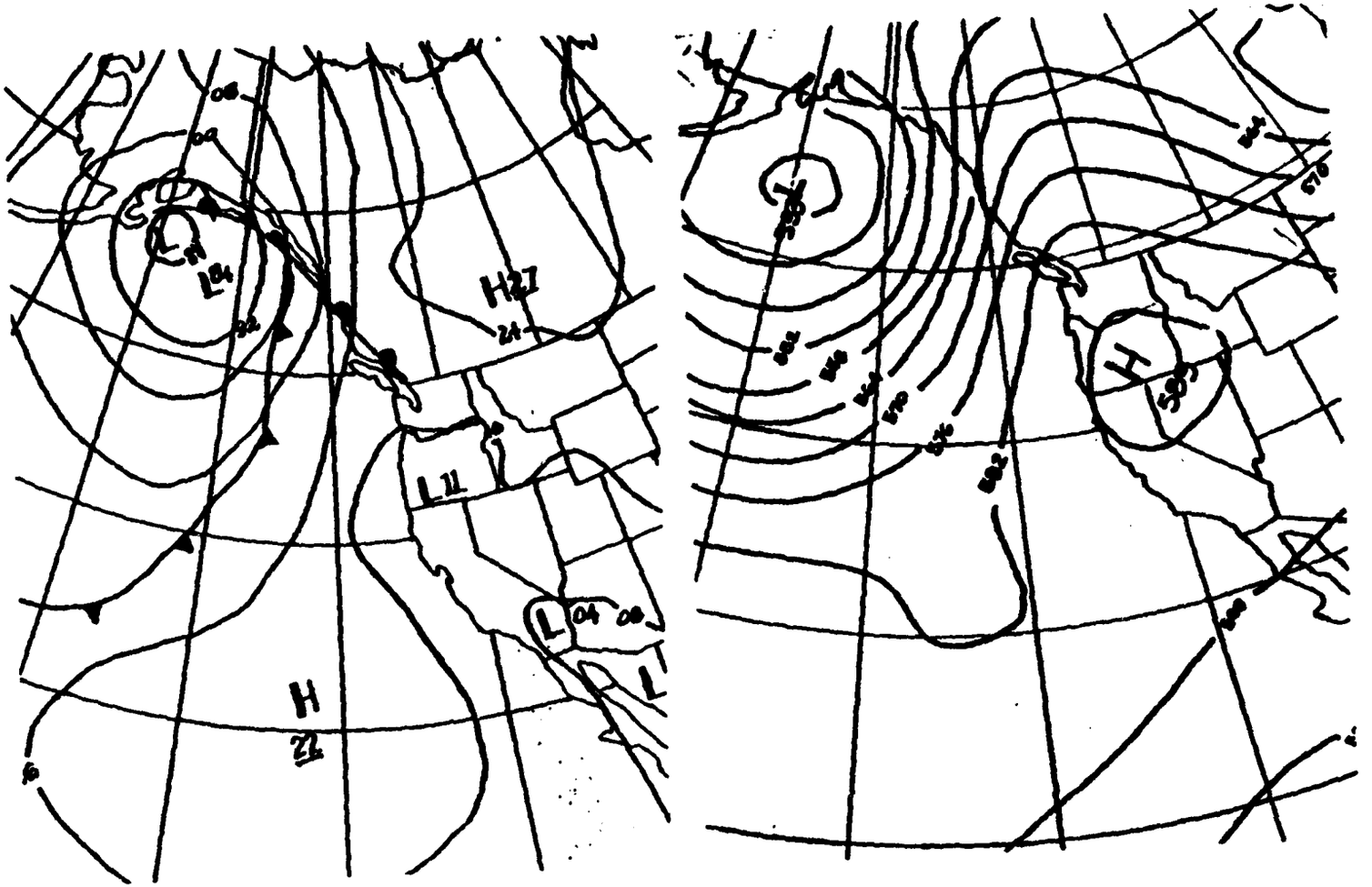

Figure 10. Same as 9 except 0000 GMT 15 Sept 1981.

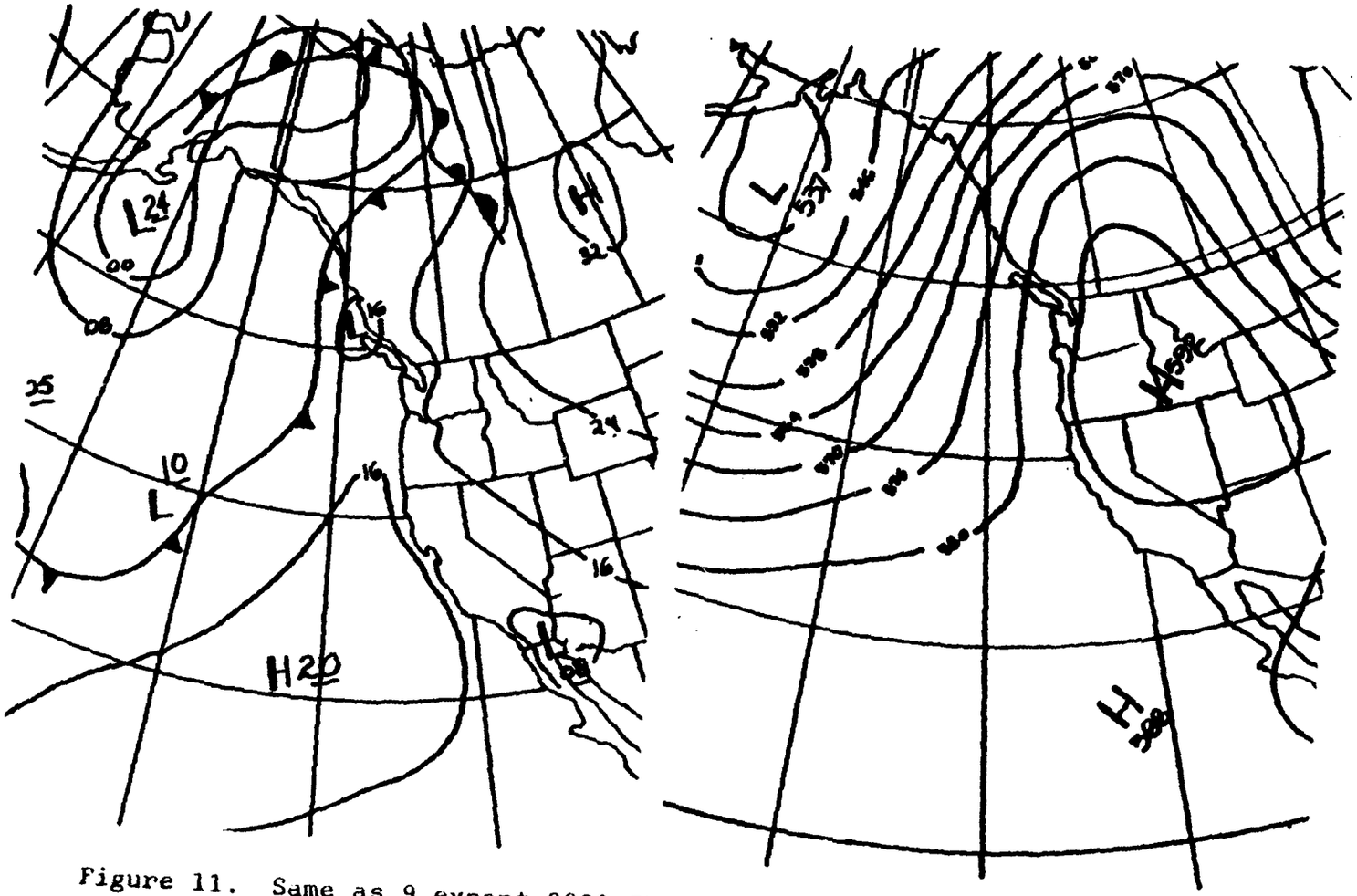

Figure 11. Same as 9 except 0000 GMT 16 Sept 1981.

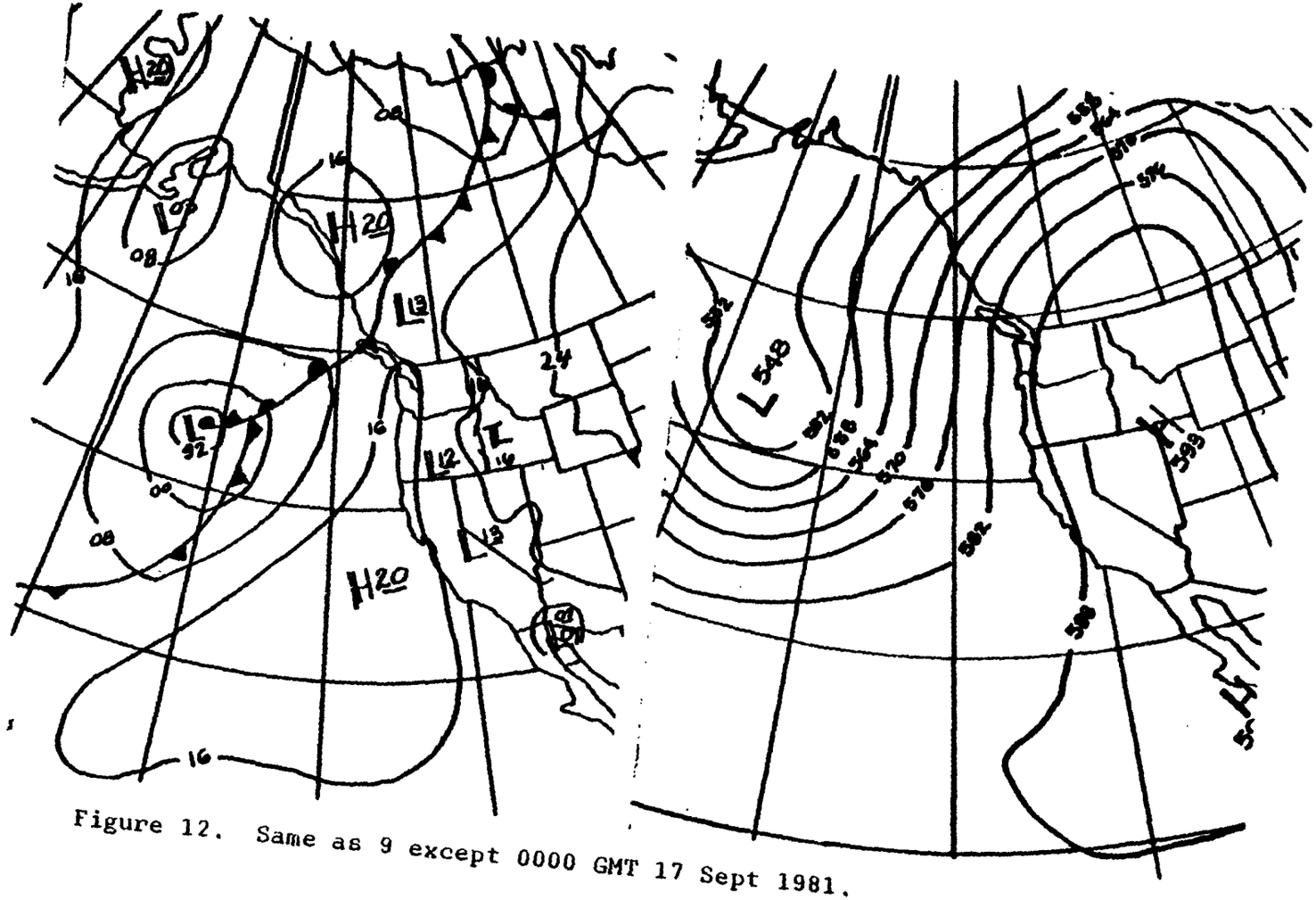

Figure 12. Same as 9 except 0000 GMT 17 Sept 1981.

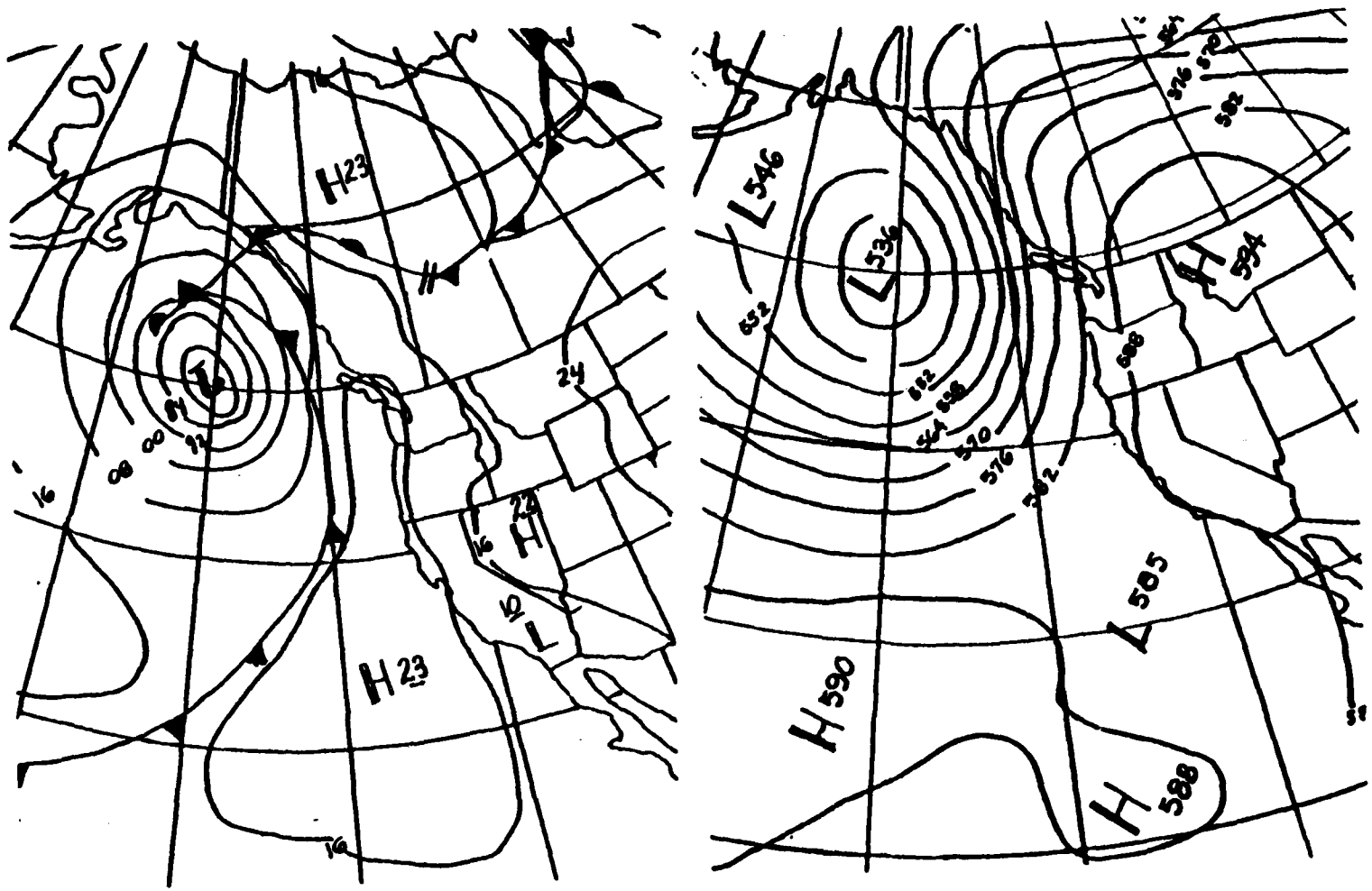

Figure 13. Same as 9 except 0000 GMT 18 Sept 1981.

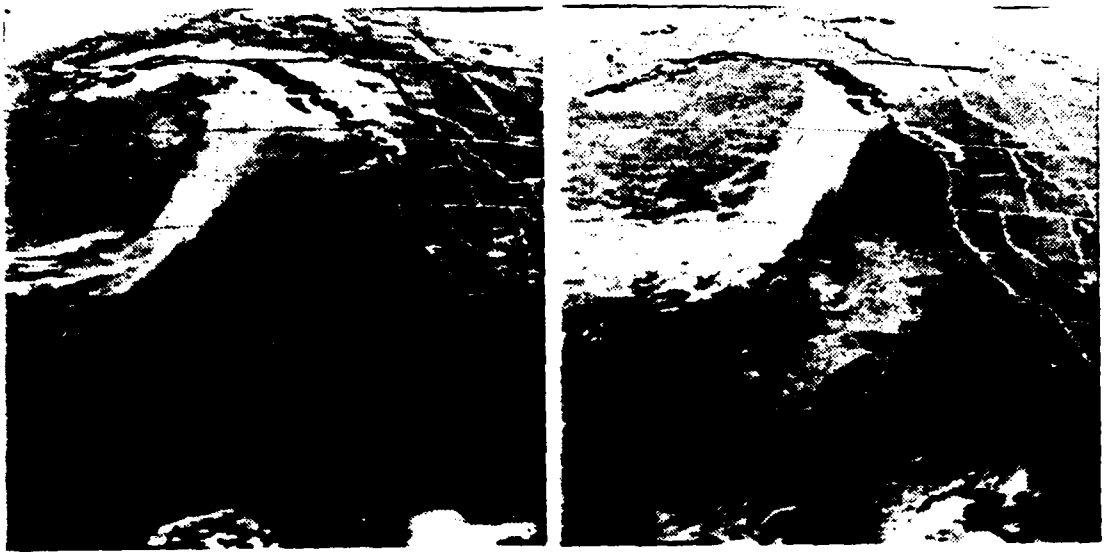

1315 GMT 14 SEP 81

1015 GMT 15 SEP 81

1015 GMT 16 SEP 81

0315 GMT 18 SEP 81

Figure 14. GOES WEST IR, Case II.

V. RESULTS

Direct measurement procedures do not exist to obtain vertical velocity values. Therefore an indirect evaluation procedure was nesessary. This was accomplished by using the RMS error (section III,E.) for model predictions of inversion height, potential temperature and specific humidity, with the large-scale vertical velocity specified by the adiabatic method, Q-method, vertical velocity equal to zero, and a persistence forecast. It is noted that the Q-method is based on measured values of the prediction variables (Eq. (1)). Therefore the model is expected to perform well with vertical velocities computed in this way.

In both cases the inversion persisted for several days. Eq. (1c) illustrates that W acts to keep a lid on the boundary layer only when subsidence ($W < 0$) is occurring since W provides only for increasing the inversion height, i.e., "detrainment" is not allowed. Then from a pragmatic view, negative vertical velocities (subsidence) are sought while positive ones are not. Large-scale subsidence is also expected, from a synoptic viewpoint in both cases, since SNI is under the summertime subtropical ridge.

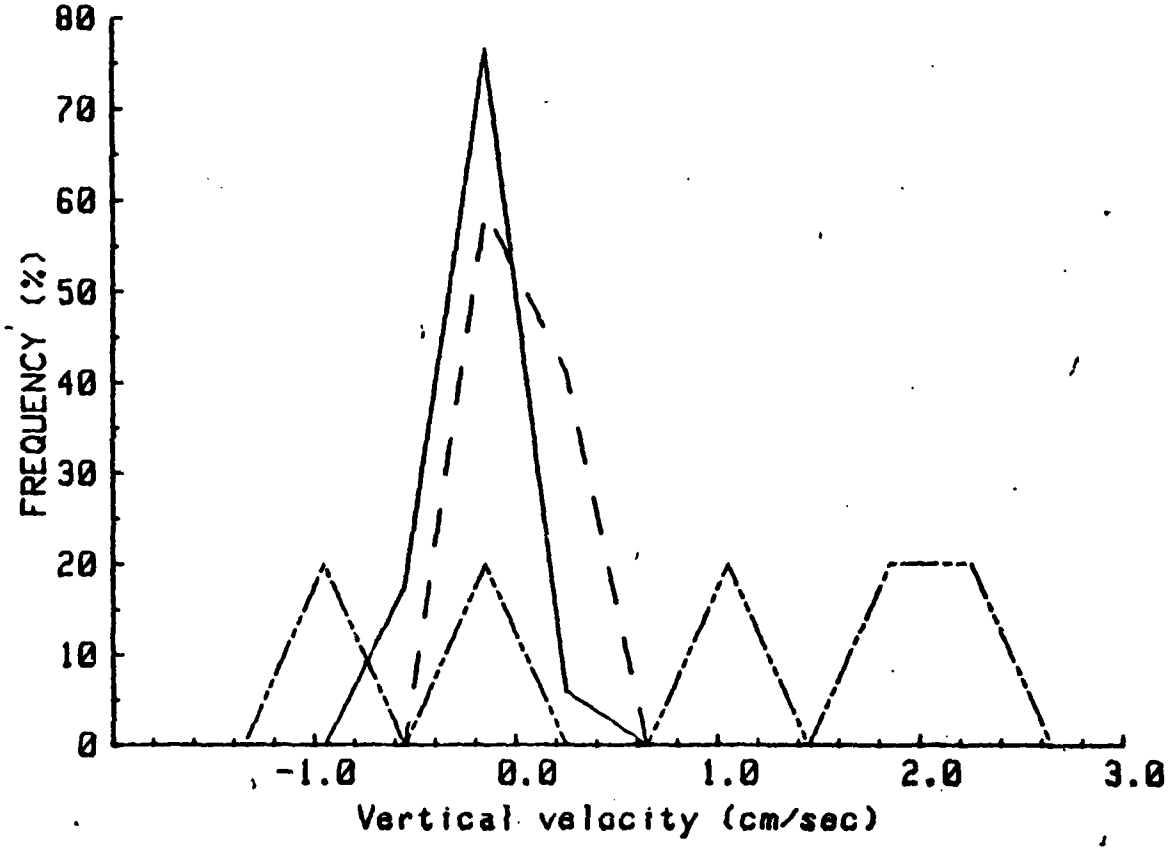

Figure 15. Frequency of occurrence of subsidence. Case I; solid: Q-method; dash: adiabatic method; double dash: kinematic method.

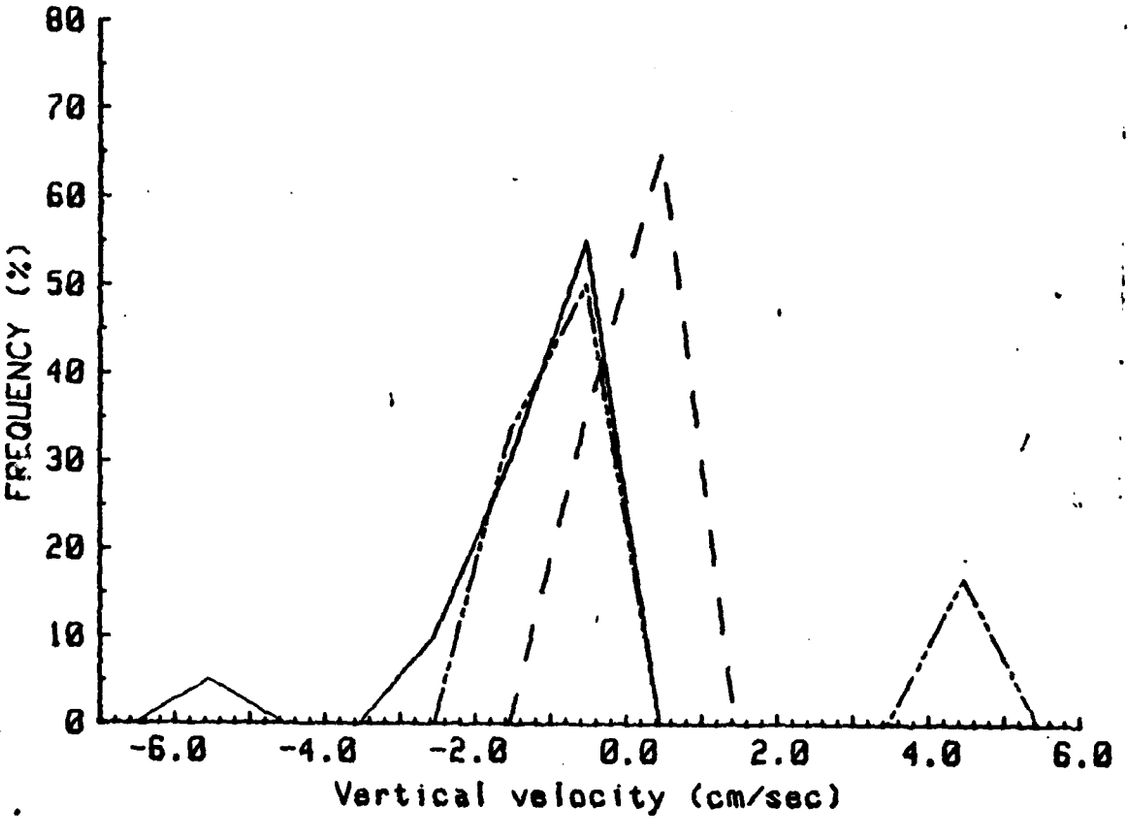

Figure 16. Same as 15 except Case II.

Table II gives the averages of the vertical velocities for each case calculated by the Q-method, the adiabatic method, and the kinematic method. The standard deviation is given in parentheses. Figs. 15 and 16 show the frequency of occurrence of calculated vertical velocity for Case I and Case II, respectively. Assuming that subsidence existed at the inversion height, the adiabatic and kinematic methods are unable to diagnose subsidence. The Q-method consistently gives subsidence where subsidence is expected. Discussion of possible sources of errors in these methods is left to a subsequent section.

TABLE II

Vertical velocity (cm/sec) comparisons

	Q-method	Adiabatic method	Kinematic method
Case I	-.26 (.14)	0.0 (.22)	1.2 (1.7)
Case II	-1.2 (1.1)	.1 (.24)	.7 (1.3)

A. DISCUSSION OF CASE I

The RMS errors for Case I appear in Table III . The average time from initialization to verification for this case was 15.6 hours. Persistence forecasts yield the least

RMS error for all variables (h, θ, and q). When the model is initialized with the large-scale vertical velocity computed by the adiabatic method or when the vertical velocity is assumed to be zero, very poor results are obtained in the inversion height prediction. Vertical velocities computed by the Q-method result in better prediction of inversion height than the adiabatic method.

TABLE III

RMS Error (Case I)

	h	θ	q
Persistence	61 m	2.2 C	.6 g/kg
W=0	167 m	2.2 C	.8 g/kg
Q-method	106 m	2.4 C	.9 g/kg
Adiabatic method	249 m	2.2 C	.7 g/kg

The large errors in the inversion height for the W=0 prediction occur because the boundary layer is constrained to growth by entrainment. The poor results of the adiabatic method are also to be expected because of two basic problems with this method. First, examination of Eq. (6) reveals that the lapse rate is assumed to be constant and the numerator is approximated by a finite difference in time over six to twelve hours. An uncertainty of ± one degree in potential temperature can lead to an uncertainty in vertical velocity of ±.5 (cm/sec), assuming nominal values of the free atmosphere lapse rate (2.5 to 5 C/Km). Since the actual

vertical velocity may be positive or negative and often on the crder .5 (cm/sec), the adiabatic method is not adequate to specify either the magnitude or the sign of the vertical velocity. Second, one must choose an appropriate time interval over which the finite difference applies. In practice the time interval was that of the rawinsonde schedule; however, the soundings must be scheduled suffiently close in time to reveal changes in sign of the tendencies of the boundary layer variables.

The Q-method also suffers from the disadvantages of finite difference in the specific humidity (dq/dt) and the inversion height (dh/dt). However, the moisture flux term has no such problem. In addition, specification of the moisture and inversion height variation with time required for these calculations does not require profiling devices such as radiosondes, but may be obtained from surface instrumentation.

B. DISCUSSION OF CASE II

Average time from initialization to verification was 14.6 hours. Table IV summarizes the results.

None of the predictions did particularly well with respect to RMS error of inversion height. The same ordering

TABLE IV

RMS Error (Case II)

	h	θ	q
Persistence	105 m	1.5 C	.7g/kg
W=0	375 m	1.5 C	1.4g/kg
Q-method	142 m	1.0 C	2.4g/kg
Adiabatic method	527 m	1.8 C	1.3g/kg

of RMS errors for inversion height prediction occurs with the vertical velocity specification methods in this case. A major difference in these results is that the model prediction of specific humidity with vertical velocity by the Q-method exhibits a 24% error, much greater than any other. This is to be expected since the average inversion height was 262m, over 40% lower than in Case I, and in Eq. (1a) the specific humidity tendency is inversely proportional to inversion height. Hence, low initial inversion heights, as was the case, coupled with predictions of inversion heights, which are too low, contribute to the over prediction of specific humidity. The Q-method yields the least RMS error in potential temperature predictions.

C. DISCUSSION OF THE KINEMATIC METHOD

Vertical velocities calculated by the kinematic method were positive more often than not as indicated in Figs. 15 and 16 . They were much larger in magnitude than those calculated by either the adiabatic method or the Q-method.

Therefore application of these to the model would have produced larger RMS errors than any presented. Two reasons for the poor results are:

- Improper specification of the bottom boundary condition.
- Small sample size for the regression approach.

Over the ocean the bottom boundary condition for Eq. (2) is that the vertical velocity equals zero at the sea surface. This is a good assumption since the surface is flat with respect to a local earth tangent plane. However, since SNI, PHTC, and VND are coastal stations, the boundary condition for Eq. (2) requires specification of the terrain (Dutton 1976).

D. CONCLUSION

Since both Case I and Case II represent small samples of observations the error statistics have little stability. However, they do suggest that vertical velocity calculated by the Q-method has the most merit as a single-station assessment. Clearly, the assumption of no vertical motion or vertical motion derived from the adiabatic method has questionable value in APBL assessments. Fig. 17 shows a model prediction with vertical velocity computed by the

Q-method. Fig. 18 is the same model run but with upward vertical velocity computed by the adiabatic method. Comparison of these figures shows the good agreement in q prediction indicated in Table III . On the other hand, the superior result of the Q-method is well illustrated by comparison of the evolution of the inversion height. The importance of diagnosing subsidence when it exists is evident by this comparison.

The assumption that SNI represents a marine environment is a possible source of error in the Q-method. Also, sea surface temperature has an indirect effect on the calculation of vertical velocity through Eq. (9). The sea surface temperatures used were obtained from the Sea Surface Thermal Analyses of the National Oceanographic and Atmospheric Administration, rather than being in-situ measurements.

Additional research is needed in specification of the large- scale forcing of the APBL. Vertical velocity by the Q-method appears promising, however larger samples must be obtained to gain statistical stability. This need not be an expensive venture. One only needs continuous measurements of sea surface temperature, air temperature, humidity and wind. That can be done on a near-continuous basis with

currently available instrumentation that does not place great demands on personnel.

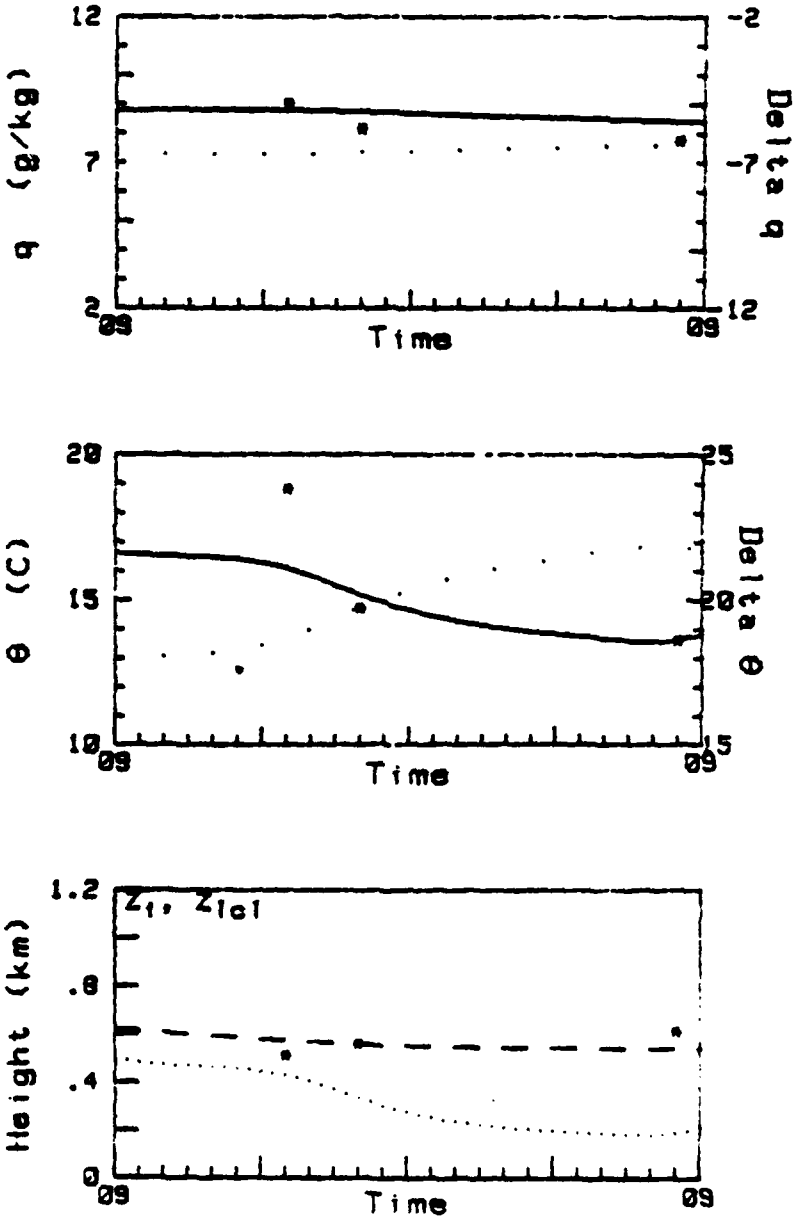

Figure 17. Model prediction: vertical velocity by Q-method, Initialization: 0900 Pacific Daylight Time, 1 September 1981. Top frame: well-mixed specific humidity (solid), jump (dotted). Middle frame: well-mixed potential temperature (solid), jump (dotted). Bottom Frame: Inversion height (dashed), lifting condensation level (dotted). Observed data are shown with an asterisk (*).

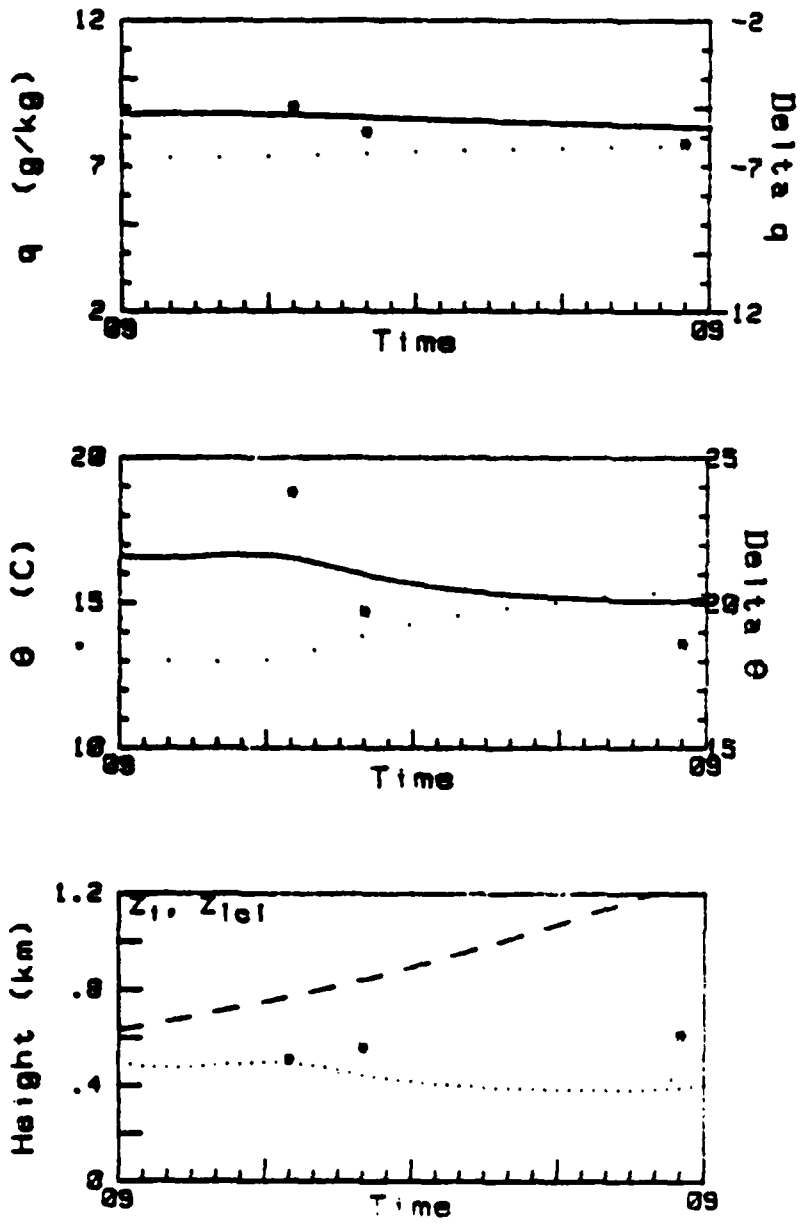

Figure 18. Same as 17 except Adiabatic Method

LIST OF REFERENCES

Battalino,T., J. Rosenthal, H. Hendon, V.R. Noonkester, 1979: "Marine/Continental History of Aerosols at San Nicolas Island during CEWCOM-78 and OSP II", TP-79-33, Pacific Missile Test Center, Point Mugu, CA.

Brower, D.A., 1982: "Marine Atmospheric Boundary Layer and Inversion Forecast Model", NPS Master's Thesis, Naval Postgraduate School, Monterey, CA., 134 pp.

Buck, A.L., 1981: "New Equations for Computing Vapor Pressure and Enhancement Factor", J. Appl. Meteor., 20, pp. 1527-1532.

Byers, H.R., 1974: General Meteorology (4th Edition), McGraw-Hill, Inc., New York, pp. 178-181.

Dutton, J.A., The Ceasless Wind 1976: McGraw-Hill, Inc., New York, pp. 321-323.

Fairall, C.W., K.L. Davidson, and G.E. Schacher, 1981: "A Review and Evaluation of Integrated Atmospheric Boundary-Layer Models", NPS-63-81-004, Naval Postgraduate School, Monterey, CA., 89 pp.

Large, W.G. and S. Pond, 1980: "Open Ocean Momentum Flux Measurements in Moderate to Strong Winds", J. Phys. Oceanogr., 11, pp. 324-331.

Lenschow, D.H., 1973: "Two Examples of Planetary Boundary Layer Modification over the Great Lakes", J. Atmos. Sci., 30, pp.568-581.

Lilly, D.K., 1968: "Models of Cloud Topped Mixed Layers under a Strong Inversion", Quart. J. Roy. Meteor. Soc., 94, pp.292-309.

Oliver, V.J. and M.B. Oliver, 1945: "Weather Analysis from Single Station Data", Handbook of Meteorology, F.A. Berry, E. Bollay, N.R. Beers, McGraw-Hill, New York, pp. 858-879.

Saucier, W.J., 1955: Principles of Meteorological Analysis, University of Chicago Press.

Stage, S.A. and Joost A. Businger, 1981: "A Model for Entrainment into a Cloud Topped Marine Boundary Layer. Part I: Model Description and Application to a Cold-air Outbreak Episode", J. Atmos. Sci., 38, pp. 2213-2229.

INITIAL DISTRIBUTION LIST

		No. Copies
1.	Defense Technical Information Center Cameron Station Alexandria, VA 22314	2
2.	Superintendent Attn: Library, Code 0142	2
	Professor C.N.K Mooers, Code 68	1
	Professor R.J. Renard, Code 63	1
	Professor K.L. Davidson, Code 63Ds	10
	Professor G.E. Schacher, Code 61Sq	10
	Professor J. Dyer, Code 61Dy	1
	Asst. Prof. R.W. Garwood, Code 68Gd	1
	Naval Postgraduate School Monterey, CA 93940	
3.	Director Naval Oceanography Division Naval Observatory 34th and Massachusetts Ave. NW Washington, D.C. 20390	1
4.	Commander Naval Oceanography Command NSTL Station Bay St. Louis, MS 39522	1
5.	Commanding Officer Naval Oceanographic Office NSTL Station Bay St. Louis, MS 39522	1
6.	Commanding Officer Fleet Numerical Oceanography Center Monterey, CA 93940	1
7.	Commanding Officer Naval Ocean Research and Development Activity NSTL Station Bay St. Louis, MS 39522	1
8.	Commanding Officer Attn: Dr. A. Weinstein	1
	Dr. A. Goroch	1
	Dr. Steven Burke	1
	Mr. Sam Brand	1
	LT Mark Schultz, USN	1
	Naval Environmental Prediction Research Facility Monterey, CA 93940	

9. Chairman, Oceanography Department 1
U.S. Naval Academy
Anapolis, MD 21402

10. Chief of Naval Research 1
800 N. Quincy Street
Arlington, VA 22217

11. Office of Naval Research (Code 480) 1
Naval Oceanography Research and Development Activity
NSTL Station
Bay St. Louis, MS 39522

12. Scientific Liaison Office 1
Office of Naval Research
Scripps Institute of Oceanography
La Jolla, CA 92037

13. Library 1
Scripps Institute of Oceanography
P.O. Box 2367
La Jolla, CA 92037

14. Library 1
Department of Oceanography
University of Washington
Seattle, WA 98105

15. Library 1
CICESE
P.O. Box 4803
San Ysidro, CA 92073

16. Library 1
School of Oceanography
Oregon State University
Corvallis, OR 97331

17. Commander 1
Oceanographic Systems Pacific
Box 1390
Pearl Harbor, HI 96860

18. Dr. C.W. Fairall 1
BDM Corporation
1340 Munras St.
Monterey, CA. 93940

19. Mr. Don Spiel 1
BDM Corporation
1340 Munras St.
Monterey,CA 93940

20. Dr. Paul Twitchell 1
Code 370C
Naval Air Systems Command
Washington, D.C. 20360

21. Dr. Alex Shantla
Code 3173
Naval Weapons Center
China Lake, CA 93555 — 1

22. Dr. Barry Katz
Code R42
Naval Surface Weapons Center
White Oak Laboratory
Silver Springs, MD 20907 — 1

23. Dr. J.H. Richter
Code 532
Naval Ocean Systems Center
San Diego, CA 92152 — 1

24. Dr. Lothar Ruhnke
Code 8320
Naval Research Laboratory
Washington, D.C. 20375 — 1

25. Mr. Herb Hitney
Naval Ocean Systems Center
Code 532
San Diego, CA 92152 — 1

26. Mr. Herb Hughes
Naval Ocean Systems Center
Code 532
San Diego, CA 92152 — 1

27. Mr. Stuart Gatham
Code 8320
Naval Research Laboratory
Washington, D.C. 20360 — 1

28. Commander
Naval Sea Systems Command
PMS-405
Washington, D.C. 20360 — 1

29. Mr. Ted Zuba
Code Air-370
Naval Air Systems Command
Washington, D.C. 20360 — 1

30. Mr. J. Rosenthal
Geophysics Division
Pacific Missile Test Center
Pt. Mugu, CA 93042 — 1

31. Dr. Michael J. Krause
AFGL/LYS
Hanscom AFB, MA 01713 — 1

32. MAJ Bob Wright
AWS/DOOE
Scott AFB, IL 62225 — 1

33. MAJ Ed Kolczynski
AWS/SYX
Scott AFB, IL 62225 — 1

34. Joel S. Davis
Defense Sciences Div.
Science Applications, Inc.
1010 Woodman Dr., Suite 200
Dayton, OH 45432 — 1

35. Mr. L. Biberman
Institute for Defense Analysis
400 Army Navy Dr.
Arlington, VA 22202 — 1

36. Dr. Richard Gomez
DELAS-EO-MO
Atmospheric Sciences Laboratory
White Sands, NM 88002 — 1

37. Dr. R. Fenn
Air Force Geophysics Laboratory
Hanscomb AFB, MA 02173 — 1

38. Mr. Glen Spaulding
MAT 72
Naval Material Command
Washington, D.C. 20362 — 1

39. Dr. Lovell Wilkens
Naval Weapons Center
China Lake, CA 93553 — 1

40. Dr. Ed Monahan
Department of Oceanography
University College
Gallway, IRELAND — 1

41. Mr. Walter Martin
Code 470, Rm 307
Office of Naval Research
800 N Quincy St.
Arlington, VA 22217 — 1

42. Dr. Gloria Patton
Office of Naval Research
1030 E Green St.
Pasadena, CA 91106 — 1

43. Dr. Warren Denner
Science Applications Inc.
2999 Monterey-Salinas Hwy
Monterey, CA 93940 — 1

44. Mr. George Hanssen 1
Science Applicationc Inc.
PO Box 1303
1710 Goodrich Dr.
McLean, VA 22102

45. Dr. Lou Goodman 1
Code 481
Office of Naval Research
Physical Oceanography
NSTL Station, MS 39529

46. CDR S.G. Colgan 1
Code 420 B
Office of Naval Research
800 N Quincy St.
Arlington, VA 22217

47. Dr. John A. Cooney 1
Department of Physics and Atmospheric Science
Drexel University
Philadelphia, PA 19104

48. Officer in Charge 1
Attn : LT J.P. Gleason, USN
NOCD, NAF Sigonella
Catania, SICILY
FPO New York 09523


END
DATE
FILMED
10-8
DTIC